Development of a Robust Thermal Management System for Lead-Acid Batteries

Article · October 2021

CITATIONS
0

READS
51

7 authors, including:

Alaa El-Sharkawy
Chrysler Group LLC.
34 PUBLICATIONS **131** CITATIONS
SEE PROFILE

Dipan Arora
Fiat Chrysler Automobiles Group
10 PUBLICATIONS **24** CITATIONS
SEE PROFILE

2021-01-0232 Published 06 Apr 2021

Development of a Robust Thermal Management System for Lead-Acid Batteries

Alaa El-Sharkawy and Dipan Arora FCA US LLC

Amr Sami and Mohamed Zaki Optumatics LLC

Krishna Guntur FCA US LLC

Citation: El-Sharkawy, A., Arora, D., Sami, A., Zaki, M. et al., "Development of a Robust Thermal Management System for Lead-Acid Batteries," SAE Technical Paper 2021-01-0232, 2021, doi:10.4271/2021-01-0232.

Abstract

Lead-acid batteries have been widely used in automotive applications. Extending battery life and reducing battery warranty requires reducing any deteriorating to battery internals and battery electrolyte. At the end of battery life, it is required to maintain at least 50% of its initial capacity [1,2]. The rate of battery degradation increases at high battery temperatures due to increased rate of electrochemical reactions and potential loss of battery electrolyte. For Lead-Acid batteries, an electrolyte solution consists of diluted sulfuric acid. Battery electrolyte/water loss affects battery performance. Water loss is caused by high internal battery temperature and gassing off due to battery electrochemistry. High temperatures, high charging rates, and over charging can cause a loss of electrolyte in non-sealed batteries. In sealed batteries, the same factors will cause an increase in temperature and pressure which can eventually result in the release of hydrogen and oxygen gases. Any loss of electrolyte resulting in part of the plates being above the electrolyte surface will result in reduced battery performance. In this paper we present an approach for design of battery thermal protection and selection of charging voltage ranges in order to reduce electrolyte (water) loss and reduce the effects of thermal degradation. Experimental bench test data were gathered at various voltages and at various battery temperatures. A mathematical model was developed to correlate water loss to the battery voltage and temperature. In order to reduce effect of external heating of the battery, thermal simulation tools are applied to assist in selecting the optimum heat shield design. The selected design along with the developed correlations are used in a vehicle level transient thermal analysis model to predict water loss and battery temperature throughout the battery life. Thus a robust approach can be followed for an improved battery thermal management and an improved battery service life and performance.

Introduction

Batteries should be designed to maintain acceptable level of battery performance during its life. Due to its location in the vehicle under-hood for most vehicles, battery internal temperature is influenced by external heat transfer factors including convection by hot air and radiation from exhaust. Internal heat generation due to electrochemical reactions contribute to the increase of electrolyte temperature as well. Internal heat generation is influenced by the battery loading and the rate of charge and discharge. During its operation, lead sulfates will form a layer on the battery electrodes. This layer can be reversed when the battery is being charged. However, with repeated cycles the sulfate layer become harder and cannot be reversed back. The sulfate deposits act as a barrier which increases internal resistance causing the battery to run hotter and causing the electrolyte to boil off. The effect of temperature on the rate of thermal degradation for battery components is exponential in nature and follows an Arrhenius model [3,4]. Therefore, it has been a common understanding that high battery temperature is the main cause for battery failure. However, recent observations indicated that battery charging strategy can strongly influence battery life. One of the main failure modes is the electrolyte/water loss or battery dry out. Water loss due to decomposition of the electrolyte is highly influenced by the charging strategy. When overcharged, a splitting of water in the electrolyte produces hydrogen and oxygen. The energy needed to produce oxygen and hydrogen is available during overcharging. Therefore, adjustment of charging as well as maintaining moderate internal battery temperatures, can reduce battery failure. In flooded batteries, lost water can be replenished by refilling, but in sealed batteries water loss can lead to dry-out and decline of performance. Due to its smaller size, auxiliary batteries are more sensitive to heat accumulation than the main battery. Figure 1 shows the effect of battery charging voltage and battery external heat exchange on battery life. Therefore, it is required to estimate the contribution of battery external heat loads and battery charging on battery life.

Previous work has been conducted [5,6] to estimate battery life due to thermal effects considering customer duty

FIGURE 1 Schematic diagram for estimation of battery life

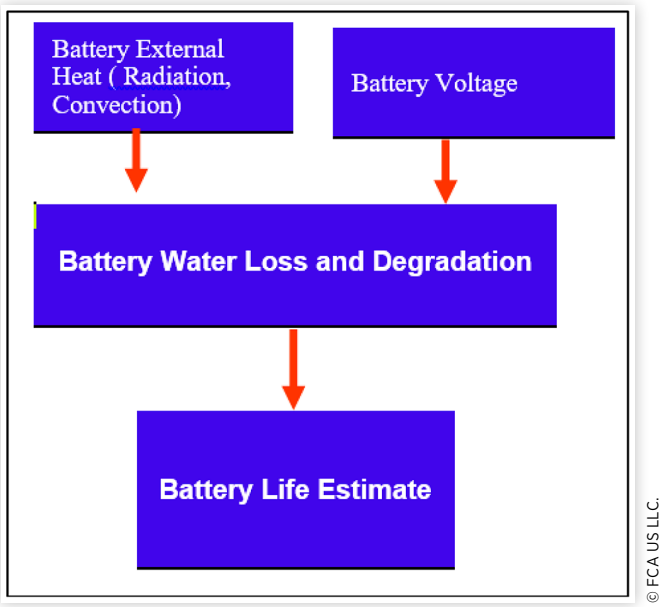

cycle and ambient weather conditions. The work in this paper, however, aims at improving this approach by incorporating an estimate for battery water loss and calculating battery life as function of both internal battery temperature and charging strategy. Therefore, the rate of water loss is calculated based on correlations derived from experimental bench test to investigate the effect of battery internal temperature and battery charging voltages. In this paper, we present:

- The experimental work using a bench test to develop correlations for water loss as function of battery internal temperature and applied voltage.
- We also present the battery thermal simulations required to estimate battery internal temperature as function of external heat exchanges and internal heat generation. The simulation allows determination of required battery shielding if external heat is the major contributor battery temperature.
- The battery model is integrated into a transient vehicle thermal analysis model (VTTA [7,8]) which can predict battery temperature for any given vehicle duty cycle.

Bench Testing

A number of auxiliary batteries was selected for the bench testing. During this test, batteries were soaked in a convection oven (Figure 2) for a duration of about 16 days. The experiment allowed testing for 3 temperature ranges and 3 different voltages as shown in the table (Figure 3). The extended test duration guarantees that all battery internal temperatures are equal to the oven temperature. Battery weights were measured frequently to determine the change in total battery weight and hence the quantity of water loss. The reduction in battery weight is therefore due to slow water loss by both electrolysis and slow evaporation.

FIGURE 2 Oven soak bench test

FIGURE 3 Thermal test parameters

12.6V	13.1V	13.5V
65C	65C	65C
75C	75C	75C
85C	85C	85C

1. **Water Loss Analysis**

The rate of water loss is expressed as a first order equation and can be expressed as follows:

$$m = m_0 * e^{-k*t} \quad (1)$$

$$k = A * e^{-E/RT} \quad (2)$$

Where k is rate coefficient, m_0 is initial water mass and m is water mass at any time t

Equation (1) can be linearized by taking the natural log of both sides as shown in equation (3)

$$Ln(m) = Ln(m_0) - (k * t) \quad (3)$$

Therefore, the rate coefficient k can be determined by plotting the natural log of the water mass versus time. This requires measuring water loss over an extended time duration for a fixed voltage and a fixed temperature.

The rate coefficient k is a strong function of temperature and can be expressed by the following Arrhenius equation [11].

$$k = A * e^{\left(-\frac{E}{RT}\right)} \quad (4)$$

Where A is the Arrhenius coefficient and E is the activation energy.The equation can also be linearized in the following form:(5)

$$Ln(k) = Ln(A) + \left(-\frac{E}{R}\right)\left(\frac{1}{T}\right)$$

Therefore, to determine the rate of water loss in an analytical form, we need to determine the value of activation energy E, at a set of voltages and battery temperature ranges. Based on test data, the following steps are followed:

1. Plot natural log of remaining water mass versus time, at a fixed voltage from which the rate coefficient k can be extracted based on equation (3) for one temperature
2. Repeat the previous step for two more temperatures at the same voltage and extract the corresponding values for the rate coefficient K.
3. Plot the natural log of K versus $(1/T)$ where T is in Kelvin, the activation energy can be extracted from the slope $(-E/R)$.
4. Repeat steps 1 to 3 for other sets of voltages. A set of values for the activation energy can be obtained for each voltage.

The range of voltages was selected to represent actual values that the battery will be operated at. The narrow range allows interpolation of activation energy for any value of voltage.

Correlations for Water loss

Test data for water loss are plotted as natural log of the remaining water mass versus time. Data are shown in Figure 4 through Figure 6 for an applied voltage of 13.5 V at battery temperatures of 65 C, 75 C and 85 C respectively. Similar charts are generated for the voltage values of 12.6 V and 13.1 V. From these charts, the value for rate coefficient K is derived as outlined in steps 1 and 2. Therefore at each voltage, 3 values of K are obtained; one value at each temperature.

The natural log of K is plotted versus $(1/T)$ for each voltage value as shown in Figures 7 through Figure 9. The slope of the fitted straight lines is equal to $(-E/R)$ where R is the universal gas constant. Therefore, 3 values for the activation energy are obtained as shown in table (Figure 10). The derived values for activation energy are applied later on to predict water loss after 500 hours of exposure for the applied voltage values of

FIGURE 4 Water loss versus time at 13.5 V and 65 C

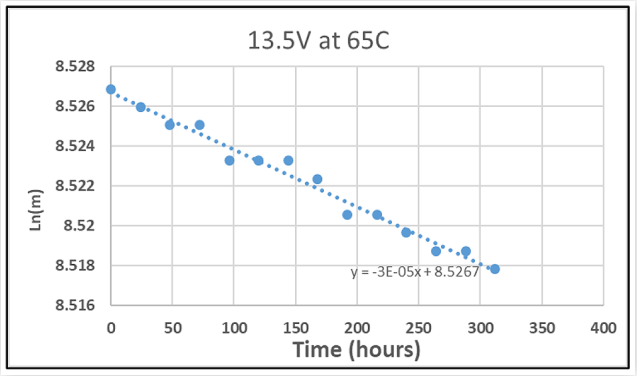

FIGURE 5 Water loss versus time at 13.5 V and 75 C

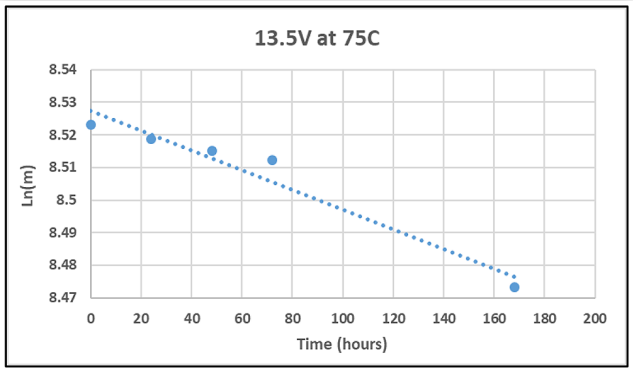

FIGURE 6 Water loss versus time at 13.5 V and 85 C

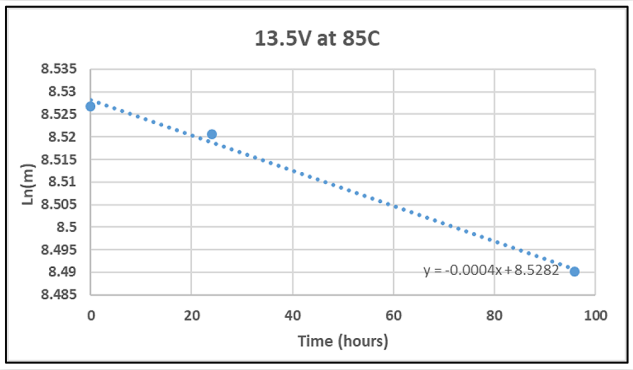

FIGURE 7 Natural log of rate coefficient versus 1/T at 12.6 V

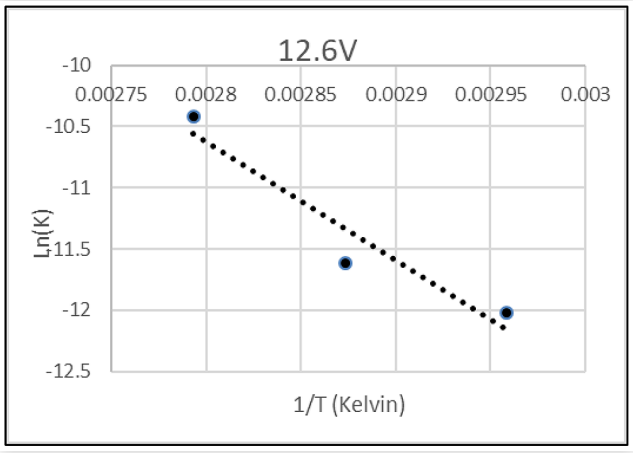

12.6 V, 13.1 V and 13.5 V as shown in Figure 11. Figure 11 indicates that the applied voltage has a major impact on the water loss. Comparing the amount of water loss at 13.1 V and 13.5 V indicates a sharp increase in water loss at 13.5 V. This suggests that careful adjustment of battery charging strategy can overcome water losses due to high internal battery temperature.

2. **Battery Thermal Models**

To understand the effect of vehicle thermal environment on battery internal temperature, a battery thermal model has

FIGURE 8 Natural log of rate coefficient versus 1/T at 13.1 V

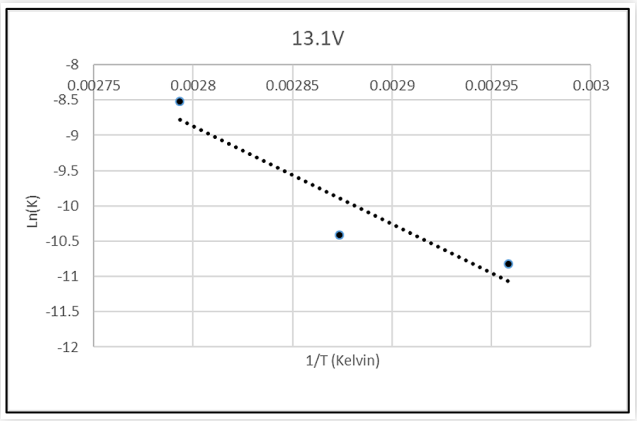

FIGURE 9 Natural log of rate coefficient versus 1/T at 13.5 V

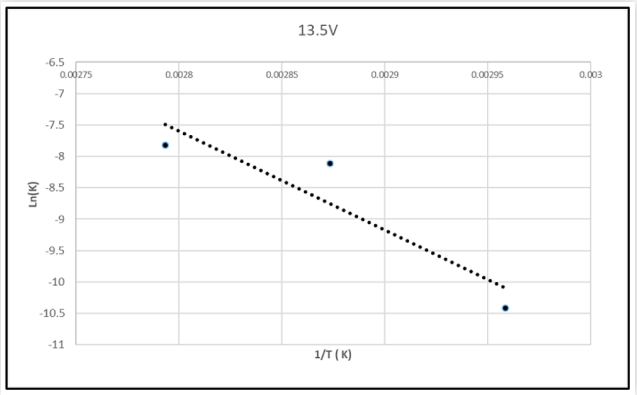

FIGURE 10 Summary of calculated activation energy values

Voltage	Temp (C)	1/T (K)	k value	Avg k	E (kJ/(mol*K))
12.6V	65	0.002959	0.000006	0.000015	**80.56**
	75	0.002874	0.000009		
	85	0.002793	0.00003		
13.1V	65	0.002959	0.00002	8.33E-05	**115.08**
	75	0.002874	0.00003		
	85	0.002793	0.0002		
13.5V	65	0.002959	0.00003	0.000243	**131.24**
	75	0.002874	0.0003		
	85	0.002793	0.0004		

been developed and applied in this study [9]. The model considers heat transfer by radiation from exhaust surfaces and by convection from surrounding air to the battery outer surface. Heat transfer by conduction from battery outer surface to battery internal surface and cells are considered in addition to internal heat generation. Heat generation which depends on the battery charging strategy is estimated for each driving condition based on existing test data. External sources of heat such as radiation and convection depend on the vehicle operating conditions. Therefore, the battery model had to be interfaced with the VTTA thermal analysis model [6,7].

FIGURE 11 Calculated water loss after 500 hours

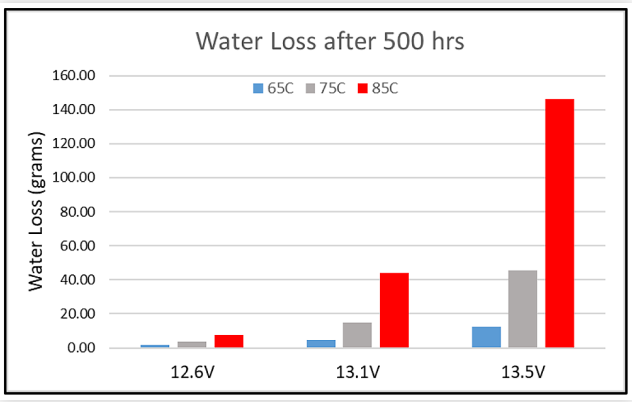

This allows the analysis of slow city traffic on the under-hood air temperature and hence on the battery temperature. At high load and high speed conditions where radiation becomes very strong heat source, the battery model can be utilized to determine the effect of exhaust surface temperature on the heat added to the battery. Therefore, selection of variety of heat shields and their impact on reduction of battery internal temperatures can be evaluated. The following section will address the detailed battery thermal model and how heat shield selection can be optimized.

Battery Thermal Models

The purpose of this model is to predict the temperature distribution of the battery's surface as well as its interiors. There are variety of heat sources that may heat up the battery. These sources include convection from the under-hood air, thermal radiation from exhaust pipes, and battery's internal heat generation. The simulation is performed using a transient thermal analysis software (VTTA). VTTA is a vehicle environment simulation that models the exhaust system of a vehicle by performing a thermal energy balance while taking into consideration heat transfer by conduction, convection, and radiation. The lead acid battery model is integrated into VTTA that includes the internal modelling of the lead acid battery. Different thermal shield designs are considered in a DOE type analysis to identify the most robust shield design that reduces the effect of external heat. The simulation is run for main and auxiliary battery internals for selected driving conditions.

Battery Internal Modelling Methodology

There exist two main methods to model a lead acid battery. The first one depends on approximating the plates inside each cell by one homogenous region with physical properties designed to produce the same thermal resistances of the individual plates lumped together. In the second method, each plate is meshed independently. In this method, more regions

are created inside each cell than in the first method in which the cell has one region only. In the first method (each cell is composed of one mesh region) the main parts to be meshed are the cells themselves, the air gap between each cell and the surrounding frame, the straps of each cell, and finally the outer frame of the battery.

Figure 12 shows an isometric view of the battery internal components. The regions in red are the air gaps between the cells (in green) and the outer frame of the battery. In yellow is the straps atop of each cell. Figure 13 shows a sample mesh representing a battery cell. All the cells of the battery are meshed in a similar manner.

As for the conductivity of the homogenous material of the cell, it can be calculated to result in a thermal resistance that is equivalent to the thermal resistance of the plates of the cell. If the thickness of plate number *i* is denoted *ti* and its conductivity is denoted *ki*, then the equivalent thermal resistance of the cell per unit area *Req* is:

$$R_{eq} = \sum_{i=1}^{n} \frac{t_i}{k_i} \tag{6}$$

Where, *n* is the number of plates. The equivalent conductivity *keq* of the assumed homogenous material of the cell is:

FIGURE 12 An isometric view of inner battery parts without the outer frame

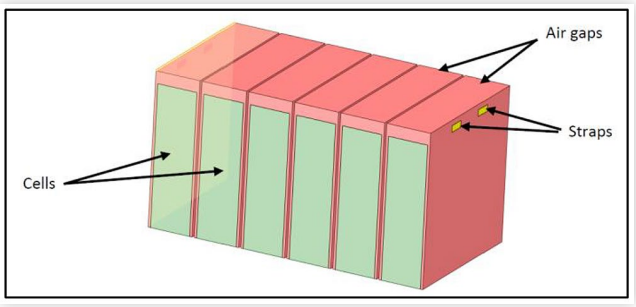

FIGURE 13 A sample mesh representing a battery cell

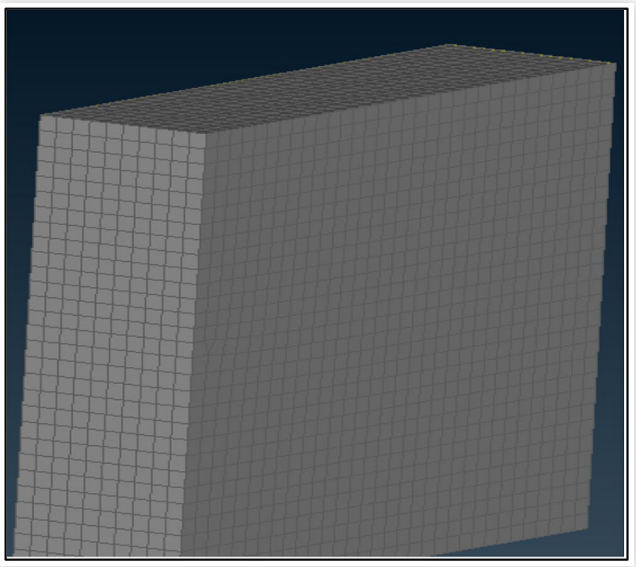

$$k_{eq} = \frac{\sum_{i=1}^{n} t_i}{R_{eq}} = \frac{\sum_{i=1}^{n} t_i}{\sum_{i=1}^{n} \left(\frac{t_i}{k_i} \right)} \tag{7}$$

The main and the auxiliary battery are divided into six cells each. Each cell consists of a negative plate, a positive plate & a separator.

Effect of Thermal Shields on Battery Internal Cell Temperature

In this study, 11 heat shield design cases have been simulated to obtain a robust shield design for minimizing the effect of external heat sources on the internal battery cells. Table 1 below shows the different material properties.

Thermal Simulation Results

The analysis for the 11 designs cases was run for a 55-minute driving scenario. The driving scenario consists of 15 minutes at steady vehicle speed, followed by an 8-minute segment of slow city traffic with frequent stops. The third segment represents a condition of uphill driving for about 22 minutes. The

TABLE 1 Thermal shield designs with varying shield material properties

	Thermal Shield Design	Thermal Conductivity W/(m.K)	Specific Heat (J/kg*K)	Density kg/m3
1	No Thermal Shield	NA	NA	NA
2	Design 1 (Without Bottom Shield)	0.034	1100	340
3	Design 2 (Without Bottom Shield)	0.042	1030	1380
4	Design 3 (Without Bottom Shield)	0.034	1350	118
5	Design 4 (Without Bottom Shield)	0.067	1782	1380
6	Design 5 (Without Bottom Shield)	0.067	1782	150
7	Design 1 (With Bottom Shield)	0.034	1100	340
8	Design 2 (With Bottom Shield)	0.042	1030	1380
9	Design 3 (With Bottom Shield)	0.034	1350	118
10	Design 4 (With Bottom Shield)	0.067	1782	1380
11	Design 5 (With Bottom Shield)	0.067	1782	150

FIGURE 14 Energy interface between the cell and its straps

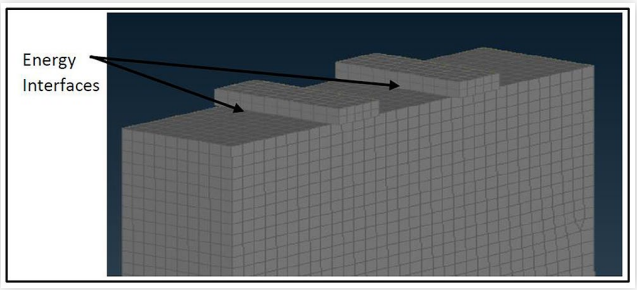

FIGURE 15 Outer frame of the battery

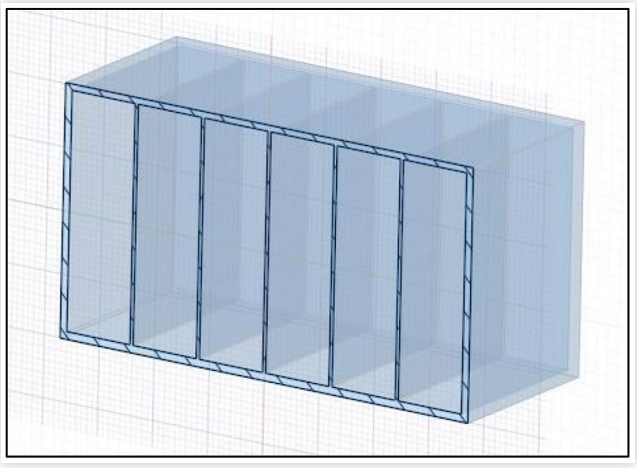

FIGURE 16 Main and auxiliary battery internal design

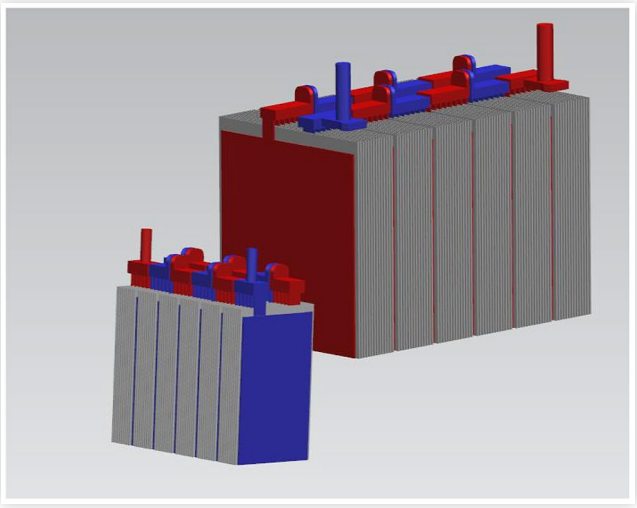

driving segments is followed by a 10-minute idle segment where the vehicle stops while the engine is still running. During the analysis the effects of external hot air and radiation from the exhaust are simulated simultaneously. Figure 17 below shows the auxiliary battery internal cell temperature for the 11 designs. The graphs below show that the no shield design has the highest internal cell temperature. While the design 3 with bottom shield is the most effective and shows

FIGURE 17 Effect of heat shields on auxiliary battery temperatures

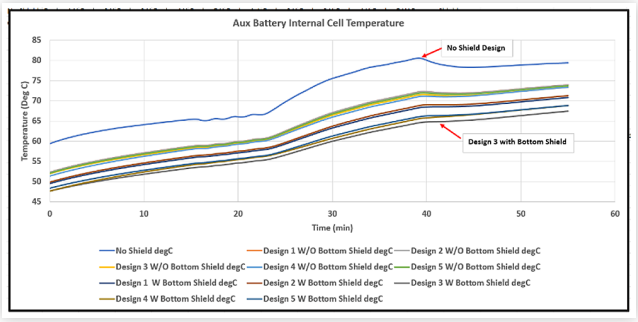

the minimum cell temperature amongst all design. Figure 18 shows the main battery internal cell temperature for the 11 designs. The graphs show that the no shield design has the highest internal cell temperature. While the design 3 with bottom shield is the most effective and shows the minimum cell temperature amongst all design.

3. **Estimation of Battery Life**

For evaluation of battery useful life, transient thermal analysis is conducted for driving scenarios which include the following:

1. City traffic
2. Freeway driving
3. Highway with trailer towing
4. Grade driving
5. Soak conditions

The selected duty cycle represents the 95Th percentile of the customer base. Each driving scenario is assigned a time percentage which varies based on the vehicle type and expected usage. The VTTA software provides transient internal battery temperature due to external heat exchange as well as internal heat generation as discussed earlier. Water loss is evaluated at each time interval based on applied voltage and internal battery temperature. A temperature histogram van be generated as shown in Figure 19 which shows the number of hours at each temperature. The histogram can assist the engineer to evaluate potential thermal issues. In addition, battery thermal degradation can be expressed as the

FIGURE 18 Effect of heat shields on main battery temperatures

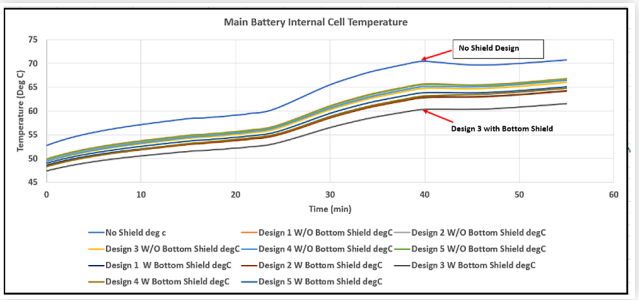

FIGURE 19 Histogram of total number of hours at each temperature

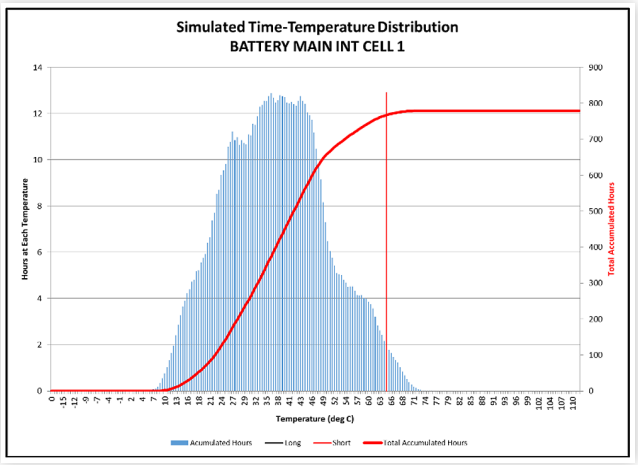

equivalent exposure time (*EET*) at any temperature using equation (8) as explained in literature [8].

$$EET = t_h \exp\left(\frac{E}{R}\left(T_l^{-1} - T_h^{-1}\right)\right) \quad (8)$$

In the above equation, t_h is the time duration above the battery temperature goal. T_l is the lower temperature (battery temperature goal). T_h is the calculated battery temperature.

During time-temperature analysis, the total number of hours above the long term are converted into a normalized number of equivalent hours *(EET)* at the goal temperature. In this example, the number of equivalent hours is below the limit of 500 hours. Therefore, it is expected that the battery will maintain its functionality throughout the expected battery service life.

Conclusion/Summary

In this paper we presented a comprehensive approach for evaluation of battery life. The approach is based on battery thermal degradation and water loss. Experimental testing was conducted to derive the correlation coefficients for water loss as function of applied voltage and battery internal temperature. A battery thermal simulation model was applied to estimate the effects of external heat sources on battery temperature. It allows the evaluation of the effect of various heat shield on battery temperature. The battery thermal model is integrated with a vehicle level thermal analysis model (VTTA). Based on previously presented topics, the battery thermal development approach should be conducted as follows:

- Evaluate the optimum thermal protection/shielding to minimize effect of external thermal effects by conducting transient thermal analysis to minimize battery internal temperature
- Estimate battery internal temperature and water loss at required operating electric loading in order to minimize the water loss. Water loss estimates can be determined using the procedure explained earlier.
- Using typical driving duty cycle, a more realistic estimate can be determined for battery life based on thermal ageing and water loss.
- The output of this analysis will be:

  a. A histogram of temperature distribution throughout the battery life, from which an estimate of battery thermal degradation can be estimated
  b. An estimate of water loss throughout vehicle life which is based on derived correlations for battery temperature and applied voltage from which an optimum charging strategy can be selected.

Therefore, a robust approach can be adopted to protect the battery for extended life and improved performance at least possible cost.

References

1. Pilatowicz, G., Budde-Meiwes, H., Shulte, D. et al., "Simulation of SLI Lead-Acid Batteries for SoC, Aging and Cranking Capability Prediction in Automotive Applications," *Journal of the Electrochemical Society* 159(9):A1410-A1419, 2012, doi:10.1149/2.019209jes.
2. Harman, C.M. and Hart, L., "Accelerated Life Cycle Testing and Analysis for Early Failure Prediction Using Two Types of Lead/Acid Batteries," *Journal of Power Sources* 37(3):363-368, 1992, https://doi.org/10.1016/0378-7753(92)85020-B.
3. Jackey, R., "A Simple, Effective Lead-Acid Battery Modeling Process for Electrical System Component Selection," 2007, doi:10.4271/2007-01-0778.
4. Liu, X., Zou, Z., Cao, X., Zhang, H., and Zhang, J., "Current Distribution on 3-D SiC Networks Lead-Acid Batteries," *Cailiao Yanjiu Xuebao/Chinese Journal of Materials Research* 18:587-592, 2004.
5. Lim, Y. and Edel, Z., "A Development of Battery Aging Prediction Model Based on Actual Vehicle Driving Pattern," SAE Technical Paper 2020-01-1059, 2020, https://doi.org/10.4271/2020-01-1059. Ceraolo, Massimo, "New Dynamical Models of Lead-Acid Batteries: Power Systems," IEEE Transactions on, 15, 1184-1190, 2000, 10.1109/59.898088.
6. El-Sharkawy, A., Arora, D., Hekal, A., Sami, A. et al., "Transient Modeling of Vehicle Under-Hood and Underbody Component Temperatures," *SAE Int. J. Mater. Manf.* 9(2), 2016, https://doi.org/10.4271/2016-01-0281.
7. El-Sharkawy, A., Sami, A., Hekal, A., Arora, D. et al., "Transient Modelling of Vehicle Exhaust Surface Temperature," *SAE Int. J. Mater. Manf.* 9(2), 2016, https://doi.org/10.4271/2016-01-0280.
8. El-Sharkawy, A. and Kamrad, J., "Sensitivity/Analysis of Material Thermal Degradation Models," *SAE Int. J. Mater. Manf.* 5(2):440-448, 2012, https://doi.org/10.4271/2012-01-0955.

9. El-Sharkawy, A., Mohamed, K., Park, Y.C., and Sami, A., "Development of a Computational Algorithm for Estimation of Lead Acid Battery Life," SAE Technical Paper 2020-01-1391, 2020, https://doi.org/10.4271/2020-01-1391.
10. Ariza, E. et al., "Modelling, Parameter Identification, and Experimental Validation of a Lead Acid Battery Bank Using Evolutionary Algorithms," *Energies* 11:2361, 2018, doi:10.3390/en11092361.
11. Barsali, S. and Ceraolo, M., "Dynamical Models of Lead-Acid Batteries: Implementation Issues," *IEEE Power Engineering Review* 22:63-63, 2002, doi:10.1109/MPER.2002.4312013.
12. Liu, X., Zou, Z., Cao, X., Zhang, H., and Zhang, J., "Current Distribution on 3-D SiC Networks Lead-Acid Batteries," *Cailiao Yanjiu Xuebao/Chinese Journal of Materials Research* 18:587-592, 2004.
13. Ceraolo, M., "New Dynamical Models of Lead-Acid Batteries," *IEEE Transactions on Power Systems* 15(4):1184-1190, 2000, doi:10.1109/59.898088.
14. Jackey, R., "A Simple, Effective Lead-Acid Battery Modeling Process for Electrical System Component Selection," SAE Technical Paper 2007-01-0778, 2007, https://doi.org/10.4271/2007-01-0778.
15. Senecal, P.K., "Numerical Optimization Using the GEN4 Micro-Genetic Algorithm Code," Engine Research Center. University of Wisconsin-Madison, August 2000.
16. Barsali, S. and Ceraolo, M., "Dynamical Models of Lead-Acid Batteries: Implementation Issues," *IEEE Power Engineering Review* 22:63-63, 2002, doi:10.1109/MPER.2002.4312013.

Nomenclature

E - Activation energy

R - Universal gas constant

EET - Equivalent exposure time

A - Arrhenius coefficient

t_h - Time duration above the material temperature goal

T_L - Material temperature goal

T_h - Measured material temperature

ISSN 0148-7191